DOI: 10.2352/ISSN.2470-1173.2016.19.COIMG-169

Spectral Resolution Enhancement of Hyperspectral Images via Sparse Representations

Konstantina Fotiadou[1,2]***, Grigorios Tsagkatakis***[1]***, Panagiotis Tsakalides***[1,2]
[1] ***ICS- Foundation for Research and Technology - Hellas (FORTH), Crete, Greece***
[2] ***Department of Computer Science, University of Crete , Greece***

Abstract

High-spectral resolution imaging provides critical insights into important computer vision tasks such as classification, tracking, and remote sensing. Modern Snapshot Spectral Imaging (SSI) systems directly acquire the entire 3D data-cube through the intelligent combination of spectral filters and detector elements. Partially because of the dramatic reduction in acquisition time, SSI systems exhibit limited spectral resolution, for example, by associating each pixel with a single spectral band in Spectrally Resolvable Detector Arrays. In this paper, we propose a novel machine learning technique aiming to enhance the spectral resolution of imaging systems by exploiting the mathematical framework of Sparse Representations (SR). Our formal approach proposes a systematic way to estimate a high-spectral resolution pixel from a measured low-spectral resolution version by appropriately identifying a sparse representation that can directly generate the high-spectral resolution output. We enforce the sparsity constraint by learning a joint space coding dictionary from multiple low and high spectral resolution training data and we demonstrate that one can successfully reconstruct high-spectral resolution images from limited spectral resolution measurements.

Introduction

Over the last decade, the demand for designing imaging systems able to reveal the physical properties of the objects in a scene of interest, has grown tremendously. To that end, Hyperspectral Imaging has emerged as a powerful technology, able to capture and process a huge amount of data, including the spatial and spectral variations of an input scene. This type of data is crucial for multiple applications, such as remote sensing, precision agriculture, food processing, medical and biological research, etc. Despite the important merits of hyperspectral imaging systems in structure identification and remote sensing, HSI acquisition and processing also comes with multiple functional constraints. Slow acquisition time, limited spectral and spatial resolution, low dynamic range, and restricted field of view, are just a few of the limitations that hyperspectral sensors exhibit, and which require further investigation.

The rapid evolution of the spectrally resolvable detector array systems that directly acquire the entire 3D data-cube through a clever combination of spectral filters and detector elements, has created an enormous excitement in the hyperspectral imaging community [1–5]. Although these systems acquire the entire spatial and spectral information directly from a single snapshot image, they unfortunately cause a reduction in spectral resolution by associating each detector/pixel with a single spectral band. The spectral resolution is a critical parameter for both visualization and subsequent procedures such as unmixing [6, 7], classification [8–10], and understanding of the variations of an input scene over time.

Traditional hyperspectral resolution enhancement approaches focus mostly on the spatial resolution of HSI systems. In the remote sensing community, conventional techniques generate the high-spatial resolution scene by fusing a low spatial resolution hyperspectral image with a high spatial resolution panchromatic image, a procedure known as pan-sharpening [11]. Another class of techniques utilizes spatio-spectral relations to improve spatial resolution [12, 13]. Furthermore, over the past decade multiple techniques have been proposed that seek to enhance the spatial resolution of multispectral imagery by exploiting the *Sparse Representations* framework [13, 14]. More specifically, the authors in [14] propose a sparsity-based approach based on the assumption that corresponding pairs of high and low spatial resolution pixel curves share the same sparse codes with respect to appropriate resolution dictionaries. In order to improve the quality of their reconstruction, a maximum a priory algorithm is utilized.

Contrary to the spatial resolution enhancement problem, in the spectral domain only a handful of techniques have been reported. The authors in [16] propose a spectral super-resolution approach applied on a generalization of the Coded Aperture Snapshot Spectral Imaging (CASSI) instrument, increasing simultaneously both the spectral and the spatial dimensions of hyperspectral scenes. Additionally, in [17] another spectral resolution enhancement is demonstrated, where the authors consider geographically co-located multispectral and hyperspectral oceanic water-color images and they enhance the limited multispectral measurements utilizing a sparsity based approach. First, they use a spectral mixing formulation and they define the measured spectrum for each pixel as the sum of the weighted material spectra. The desired high-spectral resolution spectra is expressed as a linear combination between a blurring matrix and the measured spectra. This problem is solved via a sparse-based technique.

Our proposed algorithm aims to enhance the spectral dimension, i.e., the number of acquired spectral bands, providing richer and more thorough descriptions of a scene of interest. Instead of introducing hardware solutions for spectral-resolution enhancement, such as modifying the optics or the hyperspectral sensor characteristics, the proposed scheme adheres to a signal learning paradigm, offering convenient post-acquisition processing, able to extract a richer spectral information from a limited number of spectral bands. The proposed spectral super-resolution method is formulated as an inverse imaging algorithm that recovers high-spectral information from low-spectral resolution data acquired

DOI: 10.2352/ISSN.2470-1173.2016.19.COIMG-169

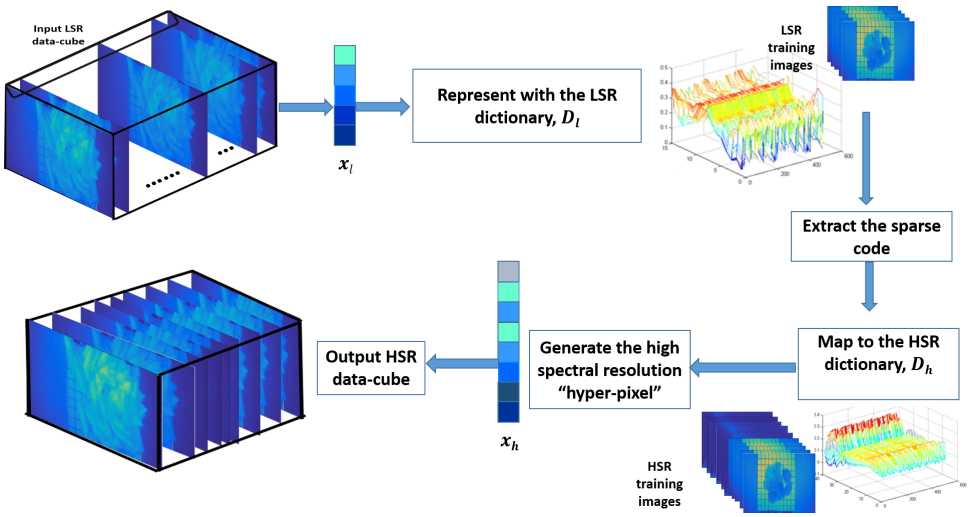

Figure 1: Block diagram of the proposed scheme: Our algorithm takes as input a hypercube acquired with a limited number of spectral bands and constructs an estimate of the full spectrum of the scene.

by the spectral detectors, by capitalizing on the *Sparse Representations* (SR) and the *joint dictionary learning* frameworks [18,19], effectively encoding the relationships between high and low spectral resolution "hyper-pixels".

Spectral Super-Resolution Using Sparsity

This work proposes a novel scheme for synthesizing a high-spectral resolution hypercube from a limited number of acquired spectral bands. More specifically, given a low-spectral resolution hyperspectral scene acquired with M spectral bands, our goal is to estimate the extended spectrum composed of N spectral bands, where $N > M$. In order to achieve this, we employ the *Sparse Representations* framework [18], which states that linear combinations between high-frequency signals can be accurately recovered from their corresponding low-frequency linear representations. The notion of sparsity has revolutionized modern signal processing and machine learning, and has lead to very impressive results in a variety of imaging problems, including super-resolution, de-nighting etc. [20,21].

Instead of observing directly the high-spectral resolution components, we work with double over-complete dictionaries, $\mathbf{D}_h$ for the high-spectral, and $\mathbf{D}_\ell$ for the low-spectral resolution scenes. The sparse code of the low-spectral resolution part in terms of $\mathbf{D}_\ell$, will be combined with the high spectral resolution dictionary to generate the desired high-spectral resolution component. Formally, given a low-spectral resolution input hypercube $\mathbf{S}_\ell$, "hyper-pixels" $\mathbf{s}_\ell \in \mathbb{R}^M$ are extracted and mapped to the low-spectral resolution dictionary matrix $\mathbf{D}_\ell \in \mathbb{R}^{M\times P}$ containing P examples. Subsequently, we seek to identify the sparse code vector $\mathbf{w} \in \mathbb{R}^P$, with respect to the corresponding low-spectral resolution dictionary matrix. Recovery of the sparse code $\mathbf{w}$ is achieved by solving the following minimization problem:

$$\min_{\mathbf{w}} ||\mathbf{w}||_0 \;\text{ subject to }\; ||\mathbf{s}_\ell - \mathbf{D}_\ell \mathbf{w}||_2^2 < \varepsilon, \tag{1}$$

where ε stands for the acceptable approximation error which is related to the added noise. This problem can be solved by a greedy strategy such as the Orthogonal Matching Pursuit algorithm [22]. Alternatively, one can replace the non-zero counting ℓ_0 pseudo-norm by its convex surrogate ℓ_1-norm: $||\mathbf{w}||_1 = \sum_i |\mathbf{w}_i|$, and solve the corresponding problem given by:

$$\min_{\mathbf{w}} ||\mathbf{s}_\ell - \mathbf{D}_\ell \mathbf{w}||_2^2 + \lambda ||\mathbf{w}||_1, \tag{2}$$

where λ is a regularization parameter, a formulation known as the LASSO problem [23]. By considering the joint training of the low and high spectral resolution dictionaries, the objective is to identify the sparse code vector that can produce both the low and the high spectral resolution representations. Consequently, assuming that such an optimal sparse code $\mathbf{w}^\star$ is found by solving Eq. 2, we recover the high spectral resolution "hyper-pixel" $\mathbf{s}_h$, by projecting $\mathbf{w}^\star$ to the high-spectral resolution dictionary, $\mathbf{D}_h$, according to:

$$\mathbf{s}_h = \mathbf{D}_h \mathbf{w}^\star \tag{3}$$

The two main challenges for the proposed spectral resolution enhancement scheme is the sufficient sparsity measure for the sparse vector $\mathbf{w}$, and the proper construction of the dictionary matrices $\mathbf{D}_\ell$, and $\mathbf{D}_h$ which will allow the sparsification of both low and higher spectral resolution data. In the following, an efficient scheme for multiple feature space dictionary learning is provided.

Coupled Dictionary Construction

Consider a set composed of high and low spectral resolution hypercubes. We assume that these scenes are realized by the same statistical process under different spectral resolution conditions, and as such, they share approximately the same sparse code with respect to their corresponding dictionaries, $\mathbf{D}_h$ and $\mathbf{D}_\ell$. A straightforward strategy to create these dictionaries is to randomly sample multiple correspondent "hyper-pixels" extracted from corresponding high and low spectral resolution training sets and use this random selection as the sparsifying dictionary. However, such a strategy is not able to guarantee that the same sparse code can be utilized among the two different representations. To overcome this limitation, we propose learning a compact dictionary from such pairs of high and low-spectral resolution data-cubes.

Given a large set of training "hyper-pixels" extracted from multiple pairs of high and low spectral resolution hyperspectral scenes $\mathbf{S}_h$ and $\mathbf{S}_\ell$, our goal is to learn a joint dictionary $\mathbf{D}_j$, taking into account both representations. Consequently, the joint dictio-

DOI: 10.2352/ISSN.2470-1173.2016.19.COIMG-169

nary learning problem is formulated as:

$$\min_{\mathbf{D}_j,\mathbf{X}} ||\mathbf{P}-\mathbf{D}_j\mathbf{X}||_2^2+\lambda||\mathbf{X}||_1, \text{ s.t } ||\mathbf{D}_j(:,i)||_2^2 \leq 1 \quad (4)$$

where $\mathbf{D}_j = \begin{bmatrix}\mathbf{D}_h \\ \mathbf{D}_\ell\end{bmatrix} \in \mathbb{R}^{(M+N)\times P}$, $M+N$ denotes the concatenated number of spectral bands for both high and low-spectrum scenarios, P is the number of dictionary atoms, and $\mathbf{P} = \begin{bmatrix}\mathbf{S}_h \\ \mathbf{S}_\ell\end{bmatrix}$ corresponds to the set of "hyper-pixels" extracted from the training pairs of high and low-spectral resolution hyperspectral images.

The problem in Eq. 4 can be efficiently solved via the K-SVD dictionary learning algorithm [24, 25], alternating between two stages, namely, the sparse coding and the dictionary update. During the sparse coding stage, the coefficients matrix $\mathbf{X}$ is estimated using any pursuit algorithm, restricting the number of non-zero elements of each sparse vector to be small. During the dictionary update step, the dictionary elements are sequentially updated via a singular value decomposition process. Fig. 1 presents the proposed system's block diagram, where we summarize the individual steps for our scheme in recovering the full spectrum from a limited number of spectral bands.

Experimental Results

This section presents quantitative performance results of our spectral resolution enhancement scheme. The synthesized spectral bands are compared against the ground truth hypercube bands and against the results obtained through cubic interpolation among the available spectral bands. Regarding the dictionary training phase, two dictionaries were prepared: (i) one sampled from NASA's Hyperion remote sensing data [26], which is applied to hyperspectral scenes with a relative structure; and (ii) one sampled from scenes acquired using IMEC's Snapshot Mosaic hyperspectral instrument [27, 28]. For each high spectral resolution training scene, we generate the corresponding low spectral resolution scene by subsampling along the spectral dimension.

In order to validate the quality of the reconstructed hypercubes, we employ the *Peak Signal to Noise Ratio* (PSNR) [29] metric formulated as: $PSNR = 10\log_{10}[L_{max}^2/MSE(x,y,\lambda)]$, where L is the maximum pixel value of the scene, MSE stands for the mean square error, and λ denotes the spectral dimension. Additionally, each estimated spectral band is compared against the corresponding ground truth spectral band in terms of the *Structural Similarity Index Metric* [30], a psychophysically modeled error metric defined as:

$$\text{SSIM}(x,y) = \frac{(2\mu_x\mu_y+c1)\cdot(2\sigma_{xy}+c_2)}{(\mu_x^2+\mu_y^2+c_1)\cdot(\sigma_x^2+\sigma_y^2+c_2)}, \quad (5)$$

where μ and σ stand for the mean value and the standard deviation, respectively.

Data Acquisition Scenarios

The proposed spectral resolution enhancement scheme is validated on both satellite and terrestrial remote sensing data. Regarding the satellite case, we conducted experiments on data acquired by NASA's Hyperion hyperspectral instrument. Due to its high spectral coverage, Hyperion scenes have been widely utilized in the remote sensing community for classification and spectral unmixing purposes. Concerning the terrestrial case, we utilized hyperspectral data acquired by IMEC's snapshot mosaic sensors. These flexible sensors multiplex optically the 3D spatio-spectral information on a two-dimensional CMOS detector array, where a layer of Faby-Perot spectral filters is deposited on top of the detector array. The hyperspectral data is initially acquired in the form of 2D mosaic images. In order to generate the 3D hypercubes, the spectral components are properly rearranged into separate spectral bands. In our experiments, we utilize the 5×5 snapshot mosaic hyperspectral sensor with 25 bands in the VNIR spectrum range ($600-875$ nm). Fig. 2 presents an example of the rose test scene acquired using the 5×5 sensor.

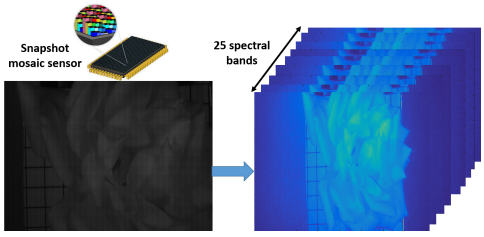

Figure 2: (Left) Rose test scene acquired by the 5×5 snapshot mosaic sensor. (Right) Individual spectral bands.

Satellite data recovery

In this scenario, we utilize hyperspectral data acquired by the Hyperion sensor. The Hyperion instrument resolves 220 spectral bands covering the range from 0.4 to 2.5 μm. In our simulations we consider only 39 spectral bands from the VNIR region with wavelengths between $437-833$ nm (bands 9-48). During the dictionary training phase, we utilized multiple hyperspectral scenes acquired by the Hyperion sensor. For the high spectral resolution dictionary, the number of bands is set to 39, while for the low spectral resolution dictionary, the down-sampling factor was set equal to 2, resulting in 20 spectral bands. Consequently, we learned two dictionaries composed of 512 atoms, from 100K randomly sampled "hyper-pixels". Fig. 3 demonstrates several recovered bands from the Hyperion sensor, along with their ground truth results. The PSNR error for the full 3D hypercube is 42.61 dB, indicating a high quality recovery.

Terrestrial data recovery

In this experiment, we apply our spectral super-resolution scheme on multiple test scenes acquired by IMEC'S 5×5 snapshot mosaic hyperspectral sensor, with a spatial resolution of 1000×2000 pixels. In the spectral domain, the acquired 3D hypercubes were subsampled by a factor of 2 and 4. The resulting dictionaries are trained from 50K randomly sampled "hyper-pixels", while the number of selected dictionary atoms was set to 512 through a validation process seeking the optimal tradeoff between quality of approximation and computational complexity. Figs. 4, 5 illustrate several reconstructed spectral bands from the *window* and the *rose* test scenes, respectively. In both experiments the sub-sampling factor was set to 2. The quantity of our reconstructions is compared against the accurate spectral bands with respect to the SSIM index. The results demonstrate that the proposed reconstructed spectral bands preserve the spectral content and exhibit high similarity with the ground truth spectral bands. Fig. 6 examines the recovery performance of the proposed synthesized rose hypercube against the interpolation reconstruction, where we illustrate the recovered 18th spectral band, along with

DOI: 10.2352/ISSN.2470-1173.2016.19.COIMG-169

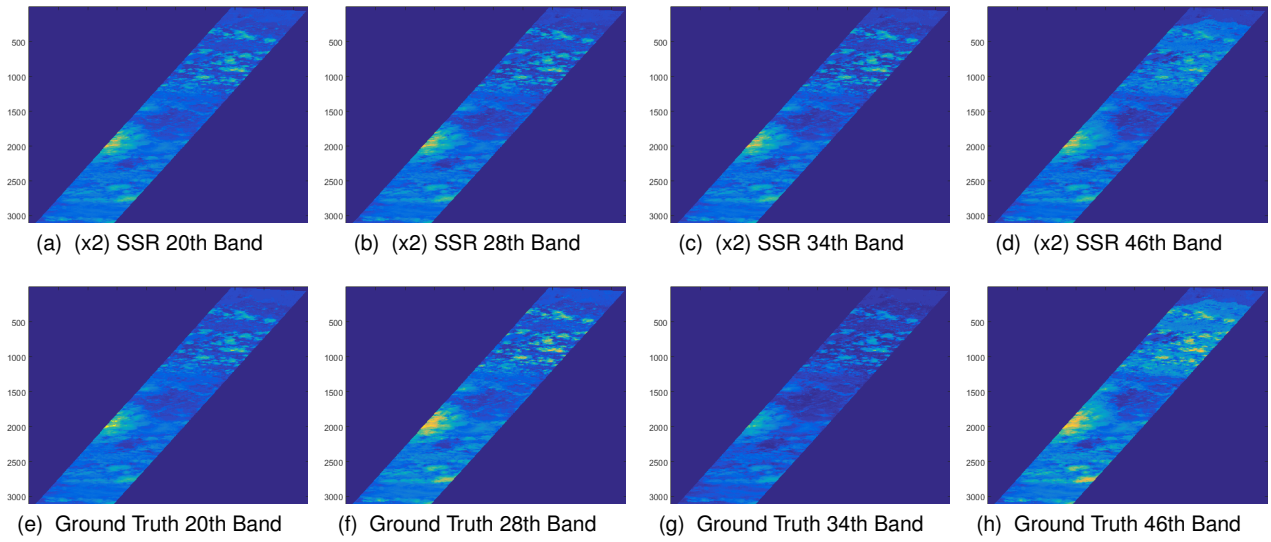

(a) (x2) SSR 20th Band (b) (x2) SSR 28th Band (c) (x2) SSR 34th Band (d) (x2) SSR 46th Band

(e) Ground Truth 20th Band (f) Ground Truth 28th Band (g) Ground Truth 34th Band (h) Ground Truth 46th Band

Figure 3: Hyperion data recovery: This experiment illustrates the capability of the proposed SSR scheme in satellite hyperspectral imagery. The full spectrum is composed of 39 bands in the VNIR region, while the sub-sampling factor is set equal to 2.

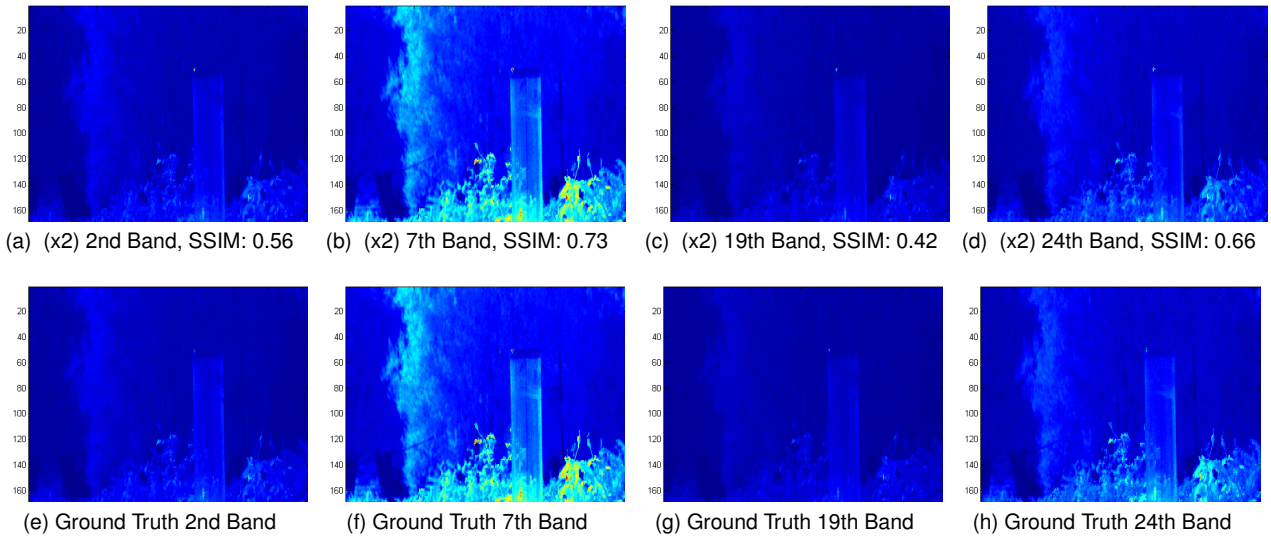

(a) (x2) 2nd Band, SSIM: 0.56 (b) (x2) 7th Band, SSIM: 0.73 (c) (x2) 19th Band, SSIM: 0.42 (d) (x2) 24th Band, SSIM: 0.66

(e) Ground Truth 2nd Band (f) Ground Truth 7th Band (g) Ground Truth 19th Band (h) Ground Truth 24th Band

Figure 4: Window reconstructed spectral bands: In this illustration the full spectrum is composed of 25 spectral bands, while the sub-sampling factor for the low-spectral resolution data-cube is 2. The proposed SSR reconstructions present high accuracy with the ground truth 3D data-cube.

the spectral signatures located at $(151, 268)$ spatial position. The results indicate that the proposed approach outperforms both visually and quantitatively the cubic interpolation procedure. Table 1 provides the PSNR reconstruction error of the proposed system, compared with the results from the cubic interpolation.

Table 1: Quantitative performance evaluation in terms of PSNR error (dB) for spectral super-resolution with magnification factor 4 and the associated ground truth frames.

Image	Rose	keys	window	Teddy-bear	Croissant
Cubic Interpolation	26.32	24.45	26.05	22.88	22.59
Proposed	**34.47**	**32.3**	**33.27**	**26.31**	**25.92**

Conclusions and Future Work

In this work, we proposed a novel post-acquisition spectral super-resolution architecture, employing the state-of-the-art mathematical modeling of *Sparse Representations* for encoding and synthesizing the relationship between high and low-spectral resolution scenes. Experimental results demonstrate the high quality of our reconstructions on both satellite and terrestrial remote sensing data. The proposed scheme can be extended to handle arbitrary low-to-high resolution enhancements by a modifica-

DOI: 10.2352/ISSN.2470-1173.2016.19.COIMG-169

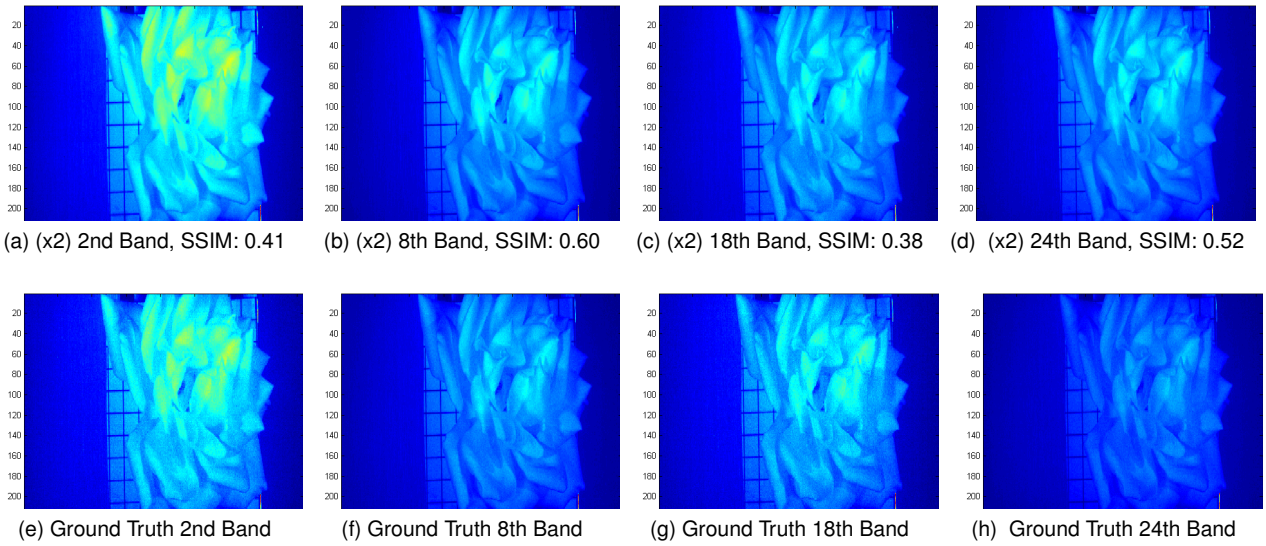

(a) (x2) 2nd Band, SSIM: 0.41 (b) (x2) 8th Band, SSIM: 0.60 (c) (x2) 18th Band, SSIM: 0.38 (d) (x2) 24th Band, SSIM: 0.52

(e) Ground Truth 2nd Band (f) Ground Truth 8th Band (g) Ground Truth 18th Band (h) Ground Truth 24th Band

Figure 5: Rose reconstructed spectral bands: In this experiment we observe the high similarity of the proposed spectral band recoveries with respect to to their original 3D full spectrum. The sub-sampling for this experiment is also set to 2.

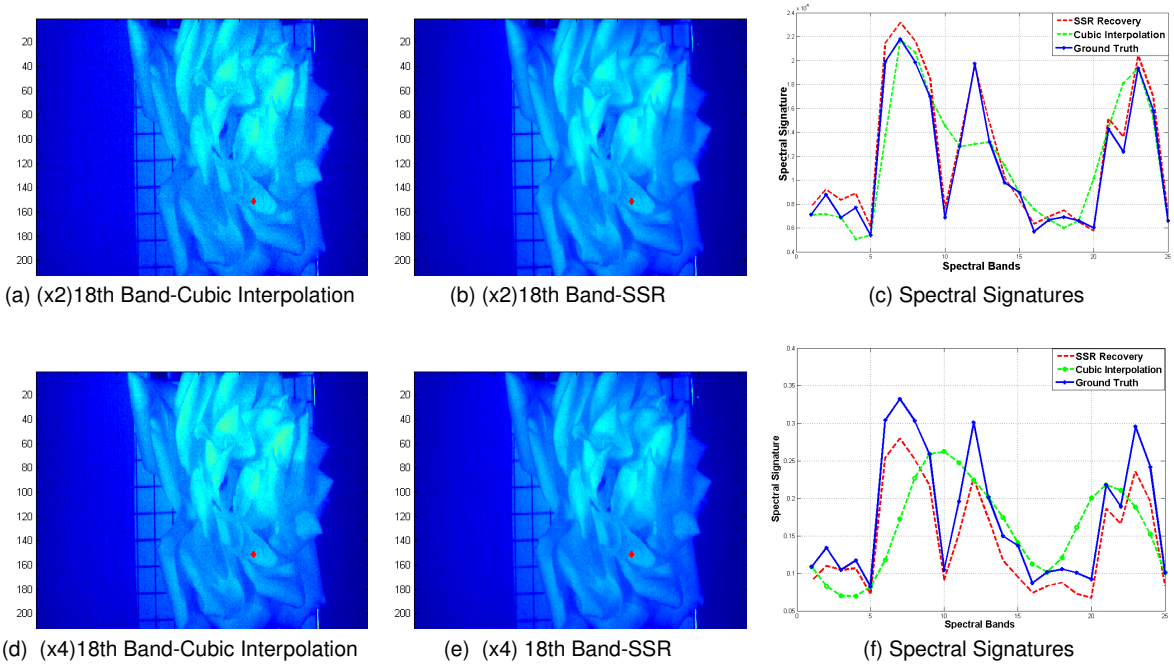

(a) (x2)18th Band-Cubic Interpolation (b) (x2)18th Band-SSR (c) Spectral Signatures

(d) (x4)18th Band-Cubic Interpolation (e) (x4) 18th Band-SSR (f) Spectral Signatures

Figure 6: Rose test scene: This experiment depicts the reconstruction performance of the proposed SSR scheme compared with the straightforward cubic interpolation procedure and the corresponding spectral signatures of each method. (Top): The sub-sampling factor is 2, and we recover the 25 full spectra from 13 input bands. (Bottom): The sub-sampling factor is 4, and the reconstructed data cube is recovered from 7 spectral bands.

tion of the joint dictionary learning process, as well as offering the capability of addressing additional sources of hyperspectral image degradation such as blurring and noise.

Acknowledgments

This work was funded by the PHySIS project, contract no. 640174, and by the DEDALE project contract no. 665044 within the H2020 Framework Program of the European Commission.

References

[1] N. Hagen, and M. W. Kudenov, Review of snapshot spectral imaging technologies, Optical Engineering 52(9), 090901-090901, (2013).

[2] A. Bodkin, A. Sheinis, A. Norton, J. Daly, S. Beaven, and J. Weinheimer, Snapshot hyperspectral imaging: the hyperpixel array cam-

DOI: 10.2352/ISSN.2470-1173.2016.19.COIMG-169

era, In SPIE Defense, Security, and Sensing, International Society for Optics and Photonics, (2009).

[3] J. M. Bioucas-Dias , A. Plaza, G. Camps-Valls, P. Scheunders, N. M. Nasrabadi, and J. Chanussot, Hyperspectral remote sensing data analysis and future challenges, Geoscience and Remote Sensing Magazine, IEEE, 1(2), pg. 6–36.(2013).

[4] G. Tsagkatakis, and P. Tsakalides, Compressed hyperspectral sensing, IS&T/SPIE Electronic Imaging, International Society for Optics and Photonics.(2015).

[5] G. Tsagkatakis, and P. Tsakalides, Recovery of Quantized Compressed Sensing Measurements. Proc. 2015 IS&T/SPIE Electronic Imaging Conference, Computational Imaging XIII, San Francisco, CA. (February 8-12 2015).

[6] N. Keshava and J. Mustard, Spectral unmixing, IEEE Signal Processing Mag., vol. 19, no. 1, pp. 44-57, (2002).

[7] J. Bioucas-Dias, A. Plaza, N. Dobigeon, M. Parente, Q. Du, P. Gader, and J. Chanussot, Hyperspectral unmixing overview, Geometrical, statistical, and sparse regression-based approaches, IEEE J. Select. Topics Appl. Earth Observ. Remote Sensing, vol. 5, no. 2, pp. 354–379, (2012).

[8] S. Kumar, J. Ghosh, and M. M. Crawford, Best-bases feature extraction algorithms for classification of hyperspectral data, IEEE Trans. Geosci. Remote Sensing, vol. 39, pp. 1368-1379, (2001).

[9] F. Melgani and L. Bruzzone, Classification of hyperspectral remote-sensing images with support vector machines,IEEE Trans. Geosci. Remote Sensing, vol. 42, no. 8, pp. 1778-1790, (2004).

[10] K. Karalas, et al: Deep learning for multi-label land cover classification, SPIE Remote Sensing. Intern. Society for Optics and Photonics. (2015).

[11] L. Alparone, L. Wald, J. Chanussot, C. Thomas, P. Gamba, L. Bruce, Comparison of pansharpening algorithms: Outcome of the 2006 GRS-S data-fusion contest. IEEE Trans. Geoscience. Remote Sensing. 45(10), pg. 3012–3021.(2007)

[12] A. Minghelli-Roman, L. Polidori, S. Mathieu-Blanc, L. Loubersac, F. Cauneau, Spatial resolution improvement by merging MERIS-ETM images for coastal water monitoring, IEEE Geoscience Remote Sensing Letters, pg. 227–231. (2006).

[13] N. Akhtar, F. Shafait, A. Mian, Sparse spatio-spectral representation for hyperspectral image super-resolution, ECCV, pg. 63–78.(2014).

[14] S.Wang, B.Wang, and Z.Zhang, Spatial resolution enhancement of hyperspectral images based on redundant dictionaries. Journal of Applied Remote Sensing 9.1(2015).

[15] Zhao, Yongqiang, et al, Coupled hyperspectral super-resolution and unmixing, Geoscience and Remote Sensing Symposium (IGARSS), 2014 IEEE International. IEEE, (2014).

[16] H. F., A. Parada, and H. Arguello, Spectral resolution enhancement of hyperspectral imagery by a multiple-aperture compressive optical imaging system, Ingeniera e Investigacion 34.3, pg. 50–55. (2014).

[17] A. S.Charles, C. J. Rozell, and N. B. Tufillaro, Sparsity based spectral super-resolution and applications to ocean water color, IGARSS 2014. Technical Abstract (2014).

[18] M. Elad, Sparse and Redundant Representations: From Theory to Applications in Signal and Image Processing. Springer (2010).

[19] M. Aharon, M. Elad, A. Bruckstein, Y. Katz, K-SVD: An Algorithm for Designing of Over-complete Dictionaries for Sparse Representations, IEEE Trans. on Signal Processing, (Volume: 54, Issue: 11), pp. 4311–4322, (Nov.2006).

[20] J. Yang, J. Wright, T. Huang, Y. Ma, Image Super-Resolution via Sparse Representations, Image Processing, IEEE Trans. on (Vol.19, Issue: 11), pp. 2861–2873. (Nov. 2010).

[21] K.Fotiadou, G.Tsagkatakis, and P. Tsakalides, Low Light Image Enhancement via Sparse Representations, Image Analysis and Recognition. Springer International Publishing, pg.84–93. (2014).

[22] J. Tropp, A. C. Gilbert, et al. Signal recovery from random measurements via orthogonal matching pursuit, IEEE Trans. on Information Theory, 53(12):4655-4666, (2007).

[23] R. Tibshirani. Regression shrinkage and selection via the lasso, Journal of the Royal Statistical Society. Serie. B (Methodological), pg 267-288, (1996).

[24] M. Aharon, M. Elad, and A. Bruckstein. K-svd: An algorithm for designing overcomplete dictionaries for sparse representation, Trans. Sig. Proc., 54(11): 4311- 4322, (Nov. 2006).

[25] M. Aharon, M. Elad,A. M. Bruckstein. K-svd and its non-negative variant for dictionary design. Optics & Photonics. International Society for Optics and Photonics, pg. 591411-591411-13. (2005).

[26] https://eo1.usgs.gov/sensors/hyperion

[27] B.Geelen, T.Nicolaas, L.Andy, A compact snapshot multispectral imager with a monolithically integrated per-pixel filter mosaic, Spie Moems-Mems. Intern. Society for Optics and Photonics. (2014).

[28] A. Lambrechts, et al, A CMOS-compatible, integrated approach to hyper-and multispectral imaging, IEEE International Electron Devices Meeting (IEDM),(2014).

[29] Singh, Arvind Kumar, et al, Quality metrics evaluation of hyperspectral images, ISPRS-International Archives of the Photogrammetry, Remote Sensing and Spatial Information, pg. 1221-1226.(2014)

[30] Z. Wang, A. C. Bovik, H. R. Sheikh, and E. P. Simoncelli. Image quality assessment: From error visibility to structural similarity, Trans. Img. Proc., 13(4):600-612, (Apr. 2004)

Author Biography

Konstantina Fotiadou *is currently pursuing the PhD degree in Computer Science from the Computer Science Department of the University of Crete. She received her M.Sc. degree in Computer Science from the Computer Science Department of the University of Crete, and B.Sc. degree in Applied Mathematics from the Department of Applied Mathematics, in 2014 and 2011 respectively. Her main research interests involve machine learning techniques for computational imaging applications.*

Grigorios Tsagkatakis *received his B.S. and M.S. degrees in Electronics and Computer Engineering from Technical University of Crete, in 2005 and 2007 respectively. He was awarded his PhD in Imaging Science from the Center for Imaging Science at the Rochester Institute of Technology, USA in 2011. He is currently a postdoctoral fellow at the Institute of Computer Science - FORTH, Greece. His research interests include signal and image processing with applications in sensor networks and imaging systems.*

Panagiotis Tsakalides *received the Diploma degree from Aristotle University of Thessaloniki, Greece, and the Ph.D. degree from the University of Southern California, Los Angeles, USA, in 1990 and 1995, respectively, both in electrical engineering. He is a Professor and the Chairman with the Department of Computer Science, University of Crete, and Head of the Signal Processing Laboratory, Institute of Computer Science, Crete, Greece. He has coauthored over 150 technical publications, including 30 journal papers. He has been the Project Coordinator in seven European Commission and nine national projects. His research interests include statistical signal processing with emphasis in non-Gaussian estimation and detection theory, sparse representations, and applications in sensor networks, audio, imaging, and multimedia systems.*